

## The Problem of Liquid Droplet Combustion—A Reexamination

B. N. RAGHUNANDAN and H. S. MUKUNDA

*Department of Aeronautical Engineering, Indian Institute of Science, Bangalore 560012, India*

The simple quasi-steady analysis of the combustion of a liquid fuel droplet in an oxidising atmosphere provides unsatisfactory explanations for several experimental observations. Its prediction of values for the burning constant ( $K$ ), the flame-to-droplet diameter ratio ( $d_f/d_s$ ) and the flame temperature ( $T_f$ ) have been found to be ambiguous if not completely inaccurate. A critical survey of the literature has led us to a detailed examination of the effects of unsteadiness and variable properties. The work published to date indicates that the gas-phase unsteadiness is relatively short and therefore quite insignificant.

A new theoretical analysis based on heat transfer within the droplet is presented here. It shows that the condensed-phase unsteadiness lasts for about 20–25% of the total burning time. It is concluded that the discrepancies between experimental observations and the predictions of the constant-property quasi-steady analysis cannot be attributed either to gas-phase or condensed-phase unsteadiness.

An analytical model of quasi-steady droplet combustion with variable thermodynamic and transport properties and non-unity Lewis numbers will be examined. Further findings reveal a significant improvement in the prediction of combustion parameters, particularly of  $K$ , when consideration is given to variations of  $c_p$  and  $\lambda$  with the temperature and concentrations of several species.  $T_f$  is accurately predicted when the required conditions of incomplete combustion or low ( $O/F$ ) at the flame are met. Further refinement through realistic Lewis numbers predicts ( $d_f/d_s$ ) meaningfully.

### INTRODUCTION

Combustion of a single fuel droplet in an oxidising atmosphere has been a subject of investigation over the past two decades. While several reviews [1–3] have appeared on various aspects of droplet combustion, there are many important features which have yet to be explained. The present paper constitutes a reexamination of the problem of liquid bipropellant droplet combustion and includes analytical studies concerning unsteadiness and variable properties.

The bulk of experimental work reported in the literature is on the combustion of suspended stationary droplets in an oxidising atmosphere [4–8]—generally air. The porous burner technique has also been in wide use [9–11]. In the above two techniques the experiments are affected by natural convection; the most striking effect being on the

shape of the diffusion flame. The effect is found to be larger in the case of porous spheres of larger diameter. Stationary suspended drops appear to undergo unsteady combustion. The zero-gravity experiments of Japanese workers [12–15] involve unsteady combustion of free fuel droplets (with no convective influence), but of these three sets of experiments, only the last is relevant to analytical models which invariably assume spherical symmetry.

The simple quasi-steady constant property analysis (SQST) of Godsave [4] is widely accepted theoretical model of liquid droplet combustion. The important analytical results of this theory which have been expanded upon by other workers [9–11] are as follows

$$\dot{m} = 4\pi(\lambda/c_p)_{av}r_s \ln(1+B), \quad (1)$$

TABLE 1

A General Comparison of Experimental Data with SQST Predictions (Material: n-heptane)

Technique	Condition	$d_0$ (mm)	$K = \frac{4\dot{m}}{\pi\rho_c d_s}$ (mm <sup>2</sup> /sec)	$\frac{d_f}{d_s}$	$T_f$ (°K)
Stationary suspended drop [2, 10]	Unsteady, natural convection	1.5	1.1	3.0	1800
Porous burner [10]	Steady, natural convection	12.0	1.8	1.35	2000
		1.5 <sup>a</sup>	1.04	1.8	
Droplet in zero-g state [14]	Unsteady				
	No convection	0.95	0.78	6-10	
Theory (SQST)	Quasi-steady				
	No convection	Any size	1.1 <sup>b</sup>	29.0	2300

<sup>a</sup> Extrapolated value.<sup>b</sup> Involves assumed transport properties.

where

$$B = [c_p(T_\infty - T_s) + H\beta/s] / Q,$$

$$(d_f/d_s) = \ln(1 + B) / \ln(1 + \beta/s), \quad (2)$$

and

$$T_f = [(c_p T_s - L + H)\beta/s + c_p T_\infty] / [c_p(1 + \beta/s)]. \quad (3)$$

Table 1 compares the predictions of SQST with representative data obtained by different experimental techniques. It is clear that the SQST predictions are not accurate, particularly with respect to flame-to-droplet diameter ratio and flame temperature.

Of the three "measurables" listed in Table 1; burning rate ( $K$  or  $\dot{m}$ ), flame position ( $d_f/d_s$ ) and flame temperature ( $T_f$ ), the prediction of  $\dot{m}$  by SQST has been most successful in obtaining support by investigators. The success of SQST has been in isolating the final functional dependence of  $\dot{m}$  on  $r_s$  or equivalently, the  $d^2$ -law which has been observed in the experiments. But the *quantitative* evaluation of  $\dot{m}/r_s$  (or  $K$ ) involves a judicious choice of thermodynamic and transport properties. One should conclude from the correlation of SQST predictions with experimental results obtained under natural convection (which is considerably larger than under zero-g [12]), that the

prediction of  $\dot{m}$  is an overestimation. In fact, if the value of  $\lambda/c_p$  is evaluated at the mean temperature between the droplet surface and the flame, the estimated burning rate will be significantly larger than that which is actually observed [7].

Similarly, the value of ( $d_f/d_s$ ) assigned by SQST is also an example of gross overestimation (see Table 1). Because of its logarithmic dependence on  $B$ ,  $d_f/d_s$  has a negligible dependence on the chosen mean thermodynamic and transport properties (Eq. 2). Furthermore,  $d_f/d_s$  is considered to be independent of the diameter of the droplet in spite of the fact that experimental observation has recorded that the initial movement of the flame is away from the droplet, followed by a gradual decrease in size as the droplet continues to shrink steadily. These aspects deserve a careful reexamination.

Referring to Table 1, the theoretically predicted values of  $T_f$  are again seen to be considerably larger than the experimental values. (The free-convection effect probably does not alter the flame temperature significantly). Although SQST predicts the adiabatic flame temperature, Eq. (3) predicts a strong dependence of  $T_f$  on  $c_p$ . While this ambiguity can be easily eliminated by considering the exact variation of  $c_p$  in the field, the inclusion of kinetics and unsteadiness becomes a necessary prerequisite for the realistic prediction of  $T_f$ .

Such discrepancies between the predictions of

SQST and the experimental results have been attributed to various factors: finite kinetics, unsteadiness of the combustion process, variations of thermodynamic and transport properties and natural convection. Of these, the effects of natural convection are not considered for the present due to the discrepancies which exist between SQST predictions and data from the zero-g experiments. An examination of finite kinetics is also hampered by uncertainties concerning details of the kinetic scheme and associated constants. Lorell et al. [16] have included the essential features of kinetics through a single-step reaction. Their numerical results show that the mass burning rate and the location of the flame front are hardly affected by variation in the activation energy (hence, the reaction rate) of the chemical reaction. The small perturbation analysis of Kassoy and Williams [17] of a single-step reaction shows that  $\dot{m}$  is affected only to an order of  $D_1^{-1/3}$  for a bimolecular reaction, where  $D_1$  is the Damköhler number. It can therefore be concluded that the explanation for the above stated discrepancies must lie either in the *non-steady nature* or the *variable properties*.

## UNSTEADY EFFECTS IN DROPLET COMBUSTION

### Earlier Investigations

The unsteady analysis of Isoda and Kumagai [13] considers only gas phase (*g*-phase) unsteadiness while neglecting radial convection terms. The solution of the conduction equation invokes the steady-state boundary conditions

$$T = T_f: \quad dT/dr = \dot{m}(H - L)/4\pi r_f^2 \quad \text{at} \quad r = r_f, \quad (4)$$

and

$$T = T_\infty \quad \text{as} \quad r \rightarrow \infty. \quad (5)$$

For the above system an analytical solution is possible which is

$$\frac{T - T_\infty}{T_f - T_\infty} = \frac{r_f}{r} \operatorname{erfc} \left[ \frac{r - r_f}{2(\alpha_g t)^{1/2}} \right]. \quad (6)$$

For the conditions (experimental *d*<sup>2</sup>-law) used by Isoda and Kumagai [13], Eq. (6) with boundary conditions (4) and (5) predicts the SQST solution for  $d_f/d_s$  at large times ( $\sim 1.5$  sec). However, the graphical-numerical technique used by the authors [13] shows a significant deviation from the above analytical solution. Another model of *g*-phase unsteadiness presented in the same report draws heavily from the experimental results and does not constitute a proper check on the theory.

The transient theory of Spalding [18] makes use of a point source at the origin where the fuel is injected into the field to simulate the burning drop. The radial convective velocity is assumed to be zero. By considering only the *g*-phase unsteadiness, Spalding has shown that the flame initially moves away from and later towards the droplet. The transient analysis as well as the results of Chervinsky [19] constitute a modification of Spalding's work. The study of the above two papers is hampered by the fact that numerical results in the physical plane are not presented.

Williams [20] has discussed the effects of unsteadiness during the pre-ignition period and established the region of validity of the quasi-steady assumption.

Kotake and Okazaki [21] have obtained numerical solutions for the general unsteady equations. The ( $d_f/d_s$ ) predicted by them is in the same range as the experimentally observed ones, but the trends of the three parameters;  $\dot{m}$ ,  $d_f/d_s$  and  $T_f$ , do not give much credibility to the correctness of their solution. Their results on  $d_s^2$  vs.  $t$  (presented in Fig. 1) show a larger initial slope and a smaller constant slope after a significantly long time. But the observed experimental trends (also shown in Fig. 1) show just the opposite, namely a smaller initial gradient which quickly approaches a constant value. The lifetime of the droplets as seen from their  $d_s^2$  vs.  $t$  graphs is very much smaller than the times observed in experiments. For instance, for a 2 mm diameter benzene droplet burning in air at 300°C, the value is about 1.8 sec. A simple calculation i.e., use of the quasi-steady expression (Eq. 1) to scale down the observed burning times at room temperature ( $t_b = d_0^2/K$ ) to that at 300°C) would show that  $t_b$  for the 2 mm droplet should be about 4.5 sec. The plots

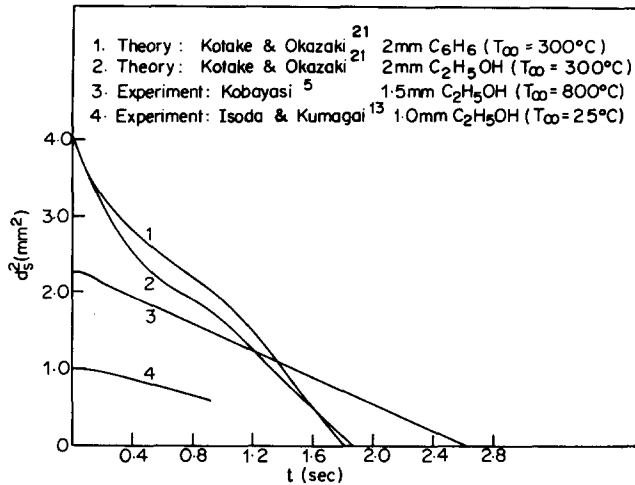


Fig. 1. Comparison of  $d_g^2$  vs.  $t$  curves in Ref. [21] with experimental results.

of Kobayasi [5] also show that at as high an ambient temperature as 800°C, a smaller droplet of benzene ( $d_0 = 1.4$  mm) will take 1.8 sec to burn out completely. Finally, the plots of  $d_f/d_g$  and  $T_f$  show a continuous increase till the end where the maximum  $T_f$  reached is much lower than the adiabatic flame temperature. These features render the numerical solution of Kotake and Okazaki [21] suspect.

A recent study on droplet evaporation by Hubbard et al. [22] suggests that the numerical results of Ref. [21] are in error. Hubbard et al. [22] have also shown that gas-phase unsteadiness is insignificant in the evaporation process. The recent report of Waldman [23] on the non-steady combustion of a droplet is based on asymptotic analysis. His results, particularly on the variation of  $d_f/d_g$  with time, show discrepancies when compared with experimental results.

### Estimation of Unsteady Periods

The ratio  $K/\alpha_g$  is an indication of the  $g$ -phase unsteady time. With typical values of  $K = 1 \times 10^{-2}$  cm<sup>2</sup>/sec and  $\alpha_g = 1$  cm<sup>2</sup>/sec, one obtains  $K/\alpha_g$  as  $10^{-2}$ , indicating that the  $g$ -phase unsteadiness lasts through a very short period. Actual calculations [24] show that the time fraction of influence is only 2-4%. The analysis of Hubbard et al. [22] support this conclusion. However, the con-

densed phase ( $c$ -phase unsteadiness ( $K/\alpha_c \sim 10$ ) can be expected to have an influence of much longer duration.

The present analysis is aimed at elucidating the influence of  $c$ -phase unsteadiness on flame characteristics. The  $g$ -phase has been taken to be quasi-steady which is justified by earlier remarks on the relative time scales.

The analysis of the  $c$ -phase is similar to the work of Wise and Ablow [25]. Their assumptions that  $T_g$  is constant throughout and that the burning rate is unaffected by gradual heating of the droplets implies that the "observables",  $K$ ,  $d_f/d_g$  and  $T_f$ , are not affected by  $c$ -phase heating—a feature which is physically inappropriate. The variation of  $T_g$  and  $\dot{m}$  with time are major aspects of the present analysis.

It is assumed that there are no chemical reactions and convective currents inside the droplet. The latter assumption is justified by the experimental observations of Hall [26] on the combustion of droplets containing suspended particles. The problem then reduces to solving the unsteady conduction equation within the droplet. The equation to be solved is

$$\frac{\partial T}{\partial t} = \frac{\alpha_c}{r^2} \frac{\partial}{\partial r} r^2 \frac{\partial T}{\partial r}, \quad (7)$$

with the conditions

$$T(0, r) = T_0 \quad \text{and}$$

$$T(t, r_s) = T_s(t); \quad \left. \frac{\partial T}{\partial r} \right|_{r=0} = 0.$$

The analytical solution for the above equation is

$$\frac{T - T_s}{T_s - T_0} = \frac{r_s}{r} \sum_{n=1}^{\infty} (-1)^n \frac{2}{n\pi} e^{-n^2 \pi^2 \alpha_c t / r_s^2} \times \sin\left(\frac{r}{r_s} n\pi\right). \quad (8)$$

Therefore, the temperature gradient at the surface is

$$\left. \frac{\partial T}{\partial r} \right|_{r=r_s} = \frac{2(T_s - T_0)}{r_s} \sum_{n=1}^{\infty} e^{-n^2 \pi^2 \alpha_c t / r_s^2}. \quad (9)$$

The above result on the  $c$ -phase temperature gradient at the surface has been obtained by treating  $r_s$  as a local constant. This solution, though different from the one obtained by Wise and Ablow [25], does not differ from it in the estimation of  $(\partial T / \partial r)|_{r_s}$  by more than 5%.

In the quasi-steady analysis, we have

$$\lambda_g \left. \frac{dT}{dr} \right|_{r_s^+} = \lambda_c \left. \frac{dT}{dr} \right|_{r_s^-} + \frac{\dot{m}}{4\pi r_s^2} L \quad (10)$$

as a boundary condition for the energy equation.

We can obtain the following expressions by including Eqs. (9) and (10) in the usual constant-property quasi-steady gas-phase analysis.

$$Y_{1s} = 1 - \eta_s / \eta_f, \quad (11)$$

$$\eta_f = 1 / (1 + \beta/s), \quad (12)$$

$$T_f = \left[ \frac{H\beta}{sc_p} + T_\infty + T_s \frac{(1 - \eta_f)}{(\eta_f - \eta_s)} \right] \frac{\eta_f - \eta_s}{1 - \eta_s}, \quad (13)$$

$$T_f - T_s = (T_s - T_0) \frac{\eta_f - \eta_s}{\eta_s \ln \eta_s} f(t, r_s) + \frac{L}{c_p} \frac{\eta_f - \eta_s}{\eta_s}, \quad (14)$$

where

$$\eta(r) = e^{-\dot{m} c_p / 4\pi \lambda_g r},$$

and

$$f(t, r_s) = -2 \frac{\lambda_c}{\lambda_g} \sum_{n=1}^{\infty} \exp\left[-\frac{n^2 \pi^2 \alpha_c}{r_s^2} t\right] \quad (15)$$

In addition we have the surface equilibrium condition

$$Y_{1s} = \exp\left[\frac{L}{R} \left(\frac{1}{T_b} - \frac{1}{T_s}\right)\right] \quad (16)$$

Once the radius ( $r_s$ ) and time ( $t$ ) are specified,  $f(t, r_s)$  (which represents the condensed-phase unsteadiness) has a unique value. Therefore, the problem is to solve the simultaneous transcendental equations (11), (13), (14) and (16) for  $Y_{1s}$ ,  $T_s$ ,  $T_f$  and  $\eta_s$ . Once we obtain  $\eta_s$ , we get the terms  $\dot{m}$  and  $d_f/d_s$  as

$$\dot{m} = 4\pi \frac{\lambda_g}{c_p} r_s \ln(1/\eta_s); \quad \frac{d_f}{d_s} = \frac{\ln(1/\eta_s)}{\ln(1/\eta_f)}. \quad (17)$$

Numerical calculations have been made for the benzene-air system by specifying  $r_s$  at time  $t$  (non-zero, but can be as small as desired). Using a suitable value of the time step ( $\sim 10^{-2} - 10^{-3}$  sec),  $r_s$  at succeeding times is evaluated using  $\dot{m}$  value as

$$r_s(t + \Delta t) = r_s(t) - \frac{\dot{m} \Delta t}{4\pi \rho_c r_s^2(t)}.$$

The results of computations are shown in Figs. 2 and 3. It must be noted that the values of  $\lambda_g$  and  $c_p$  are to be chosen such that the total burning time and the flame temperature are reasonably predicted. The duration of unsteadiness as a fraction of total burning time does not depend on the choice of  $\lambda_g$  and  $c_p$ .

From Fig. 2 it is seen that the plot of  $(d/d_0)^2$  vs.  $t$  is linear except for a short time in the beginning where it has a smaller slope. Similarly,  $d_f/d_s$  attains values close to the SQST prediction ( $\sim 29.5$ ) in a very short time. The time period dur-

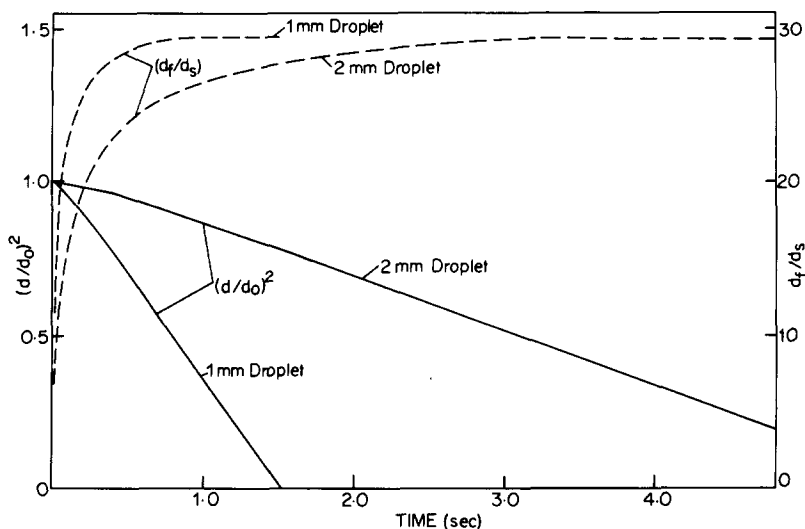


Fig. 2. Variation of  $(d/d_0)^2$  and  $(d_f/d_s)$  with time for benzene droplets—unsteady analysis.

ing which the results are significantly different from the SQST is around  $0.2t_b$  both for 1 mm and 2 mm benzene droplets. During the short unsteady period the departure from linearity of  $(d/d_0)^2$  vs.  $t$  plot cannot be easily discerned, just as in the experimental data which also show similar trends (Fig. 1).

The variations of  $\dot{m}$  and  $r_f$  during the life of a 2 mm droplet are shown in Fig. 3. The mass burning rate increases initially (though the droplet radius decreases) owing to the increasing  $T_s$  and decreasing  $\partial T/\partial r|_{r_s}$ . After the unsteady period,  $\dot{m}$  decreases gradually while at every instant remaining proportional to the instantaneous radius. The flame radius follows  $\dot{m}$  in its trend. The point of maximum ( $\sim 1.0$  sec) denotes the onset of the steady-state. In the unsteady period the term  $f(t, r_s)$  (Eq. 15) falls from 54 to 2, showing virtually no sensible enthalpy transfer into the condensed-phase at the end of the period. Other parameters,  $T_s$ ,  $T_f$  etc., also attain values obtainable from the SQST as the transient vanishes.

Experimentally, the unsteadiness is observed mainly through the flame movement. The zero-g results of Kumagai et al. [14] show that  $d_f$ -maximum occurs at about 0.4 sec from ignition for an n-heptane droplet ( $d_0 = 1$  mm) for which  $K = 0.78$  mm<sup>2</sup>/sec. The total burning time for this droplet

is 1.27 sec though data recording is made only for a short period of 0.5 sec. Hence, the peak in  $d_f$  occurs at  $0.31t_b$ . Similar deductions can also be made from the results in Refs. [13] and [15] ( $d_f$ -maxima occur at  $0.28$ - $0.32t_b$ ). Considering that there may be additional unsteadiness in the said experiments because of initial release of the chamber causing convective currents and that the above analysis includes certain approximations, the predictions on flame movement appear reasonable.

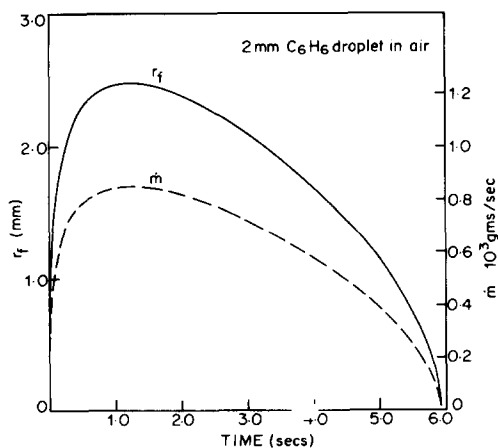


Fig. 3. Mass burning rate ( $\dot{m}$ ) and flame radius ( $r_f$ ) as functions of time—unsteady analysis.

Thus we can conclude that the unsteadiness in droplet combustion lasts only through 20–25% of the total burning time, unsteadiness being relevant only for obtaining time variation of  $d_f$  and  $d_s^2$  and not for the asymptotic steady values. In conclusion, the discrepancies between experimental observations and the predictions of constant property quasi-steady analysis cannot be attributed to unsteadiness. We shall now examine the effect of the variable nature of thermodynamic and transport properties.

### VARIABLE PROPERTIES IN COMBUSTION OF DROPLETS

The thermodynamic and transport properties involved in the theoretical analysis of droplet combustion are specific heat at constant pressure ( $c_p$ ), thermal conductivity ( $\lambda$ ) and diffusion coefficient. In actuality these vary with both concentrations and temperature and since the combustion of a droplet involves strong variations of these quantities, such variations may be expected to affect the overall results significantly.

#### Earlier Investigations

Goldsmith and Penner [27] introduced the variation of fuel specific heat and thermal conductivity as linear functions of temperature into the simple theory of Godsave [4] and extended it to obtain the relation for flame position and temperature. However, the calculated values of burning constants are much too high. This is evidenced by the fact that they correspond to values derived from experiments with natural convection [28] which enhances the burning rate. Similarly, the estimated flame temperatures are also very high even when compared with constant property predictions. The linear variation of specific heat with temperature ( $c_p = a_1 + b_1 T$ ) employed by them [27] is compared with the values from Svehla's tables [29] in Fig. 4. It is evident that the law is unrealistic, particularly when the flame temperature obtained is as high as 3400°K. In addition, the results for  $d_f/d_s$  seem to be extremely sensitive to varia-

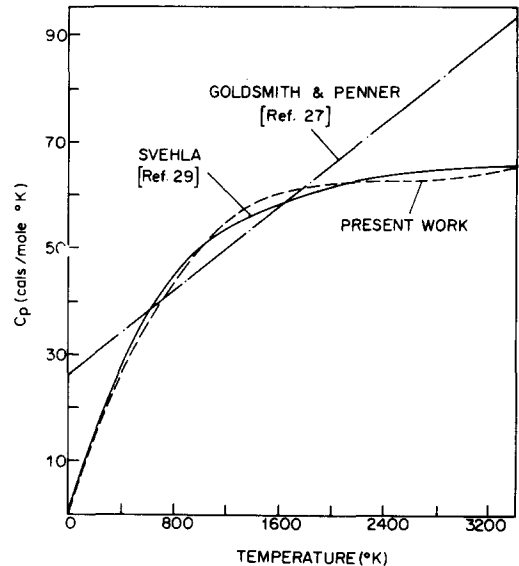


Fig. 4.  $c_p$ -variation with temperature for benzene.

tions in  $b_1$ , particularly in the range  $0 \leq b_1 \leq 10^{-4}$  (see Fig. 5). A small gradient in the  $c_p - T$  relation produces a surprisingly large change in  $d_f/d_s$ .

Williams [30] has obtained a set of relations for combustion parameters whereby arbitrary dependences of  $D$  and  $c_p$  on temperature are allowed. (Lewis number is taken as unity). The merits of this work in comparison with experimental results are not easily seen as no numerical results are presented.

Kassoy and Williams [31] have introduced  $\lambda$  and  $D$  variation (with temperature only) in their analysis using singular perturbation technique, but have considered  $c_p$  as a constant. They have used a value of unity for the stoichiometric ratio (which is seldom true for a liquid hydrocarbon-oxygen system) and therefore, the predicted low  $d_f/d_s$  ( $\sim 10$ ) is not surprising. At such  $O/F$  even SQST predicts low values of  $d_f/d_s$  (Eq. 2). It may be noted that in their modified flame surface theory, Peskin and Wise [32] have also used a value of unity for  $O/F$  and consequently have arrived at low  $d_f/d_s$  ( $\sim 10$ ).

None of the earlier investigators have incorporated the detailed variation of  $c_p$  and  $\lambda$  (with temperature and concentration). The effect of the

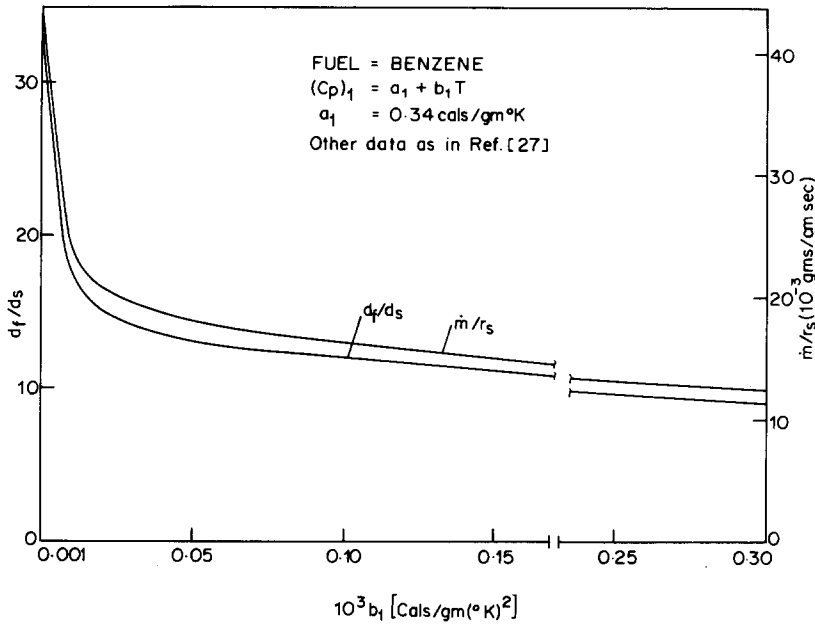


Fig. 5. Dependence of  $d_f/d_s$  and  $m/r_s$  on  $b_1$  in the analysis of Goldsmith and Penner [27].

Lewis number ( $=\rho D c_p/\lambda$ ) and of low ( $O/F$ ) at the flame are features well worth examining in addition to the introduction of variable properties in SQST.

### An Analysis with Variable Properties

The present model considers a quasi-steady combustion process with the Lewis numbers in the inner and outer zones as constants but not necessarily equal. The specific heat and thermal conductivity are considered as functions of temperature and concentrations of various species, namely fuel, oxidiser, products and inert. The assumptions shared with other quasi-steady analyses are spherical symmetry, Burke-Schumann kinetics, single-step reaction, quasi-steady state and the absence of radiative heat transfer, natural convection and thermal diffusion.

The species and energy conservation equations can be written as

$$\rho v \frac{dY_i}{dr} - \frac{1}{4\pi r^2} \frac{d}{dr} \left( 4\pi r^2 \rho D_i \frac{dY_i}{dr} \right) = \dot{w}_i''', \quad i = 1, 4 \quad (18)$$

and

$$\begin{aligned} \rho v \frac{dh_s}{dr} - \sum_{i=1}^4 h_{si} \frac{1}{4\pi r^2} \frac{d}{dr} \left( 4\pi r^2 \rho D_i \frac{dY_i}{dr} \right) \\ - \sum_{i=1}^4 \rho D_i \frac{dh_{si}}{dr} \frac{dY_i}{dr} - \frac{1}{4\pi r^2} \frac{d}{dr} \left( 4\pi r^2 \lambda \frac{dT}{dr} \right) \\ = - \sum_{i=1}^4 h_i \dot{w}_i''', \end{aligned} \quad (19)$$

where

$$h_s = \sum_{i=1}^4 h_{si} Y_i = \sum_{i=1}^4 Y_i \int_{T_{ref}}^T c_{pi} dT.$$

Combining Eqs. (18) and (19) and simplifying, the

energy equation takes the form

$$\begin{aligned} & \frac{d}{dr} \left( 4\pi r^2 \lambda \frac{dT}{dr} \right) + \frac{dT}{dr} \\ & \times \left[ 4\pi r^2 \sum_{i=1}^4 \rho D_i c_{pi} \frac{dY_i}{dr} - \dot{m} c_p \right] \\ & = \sum_{i=1}^4 4\pi r^2 h_i \dot{w}_i''' , \end{aligned} \quad (20)$$

where  $\dot{m} = 4\pi r^2 \rho v$  and  $h_i = h_{si} + h_i^o$ .

Making use of the transformation

$$\eta = \exp \left[ \int \frac{\dot{m} c_p}{4\pi r^2 \lambda} dr \right] ,$$

and writing  $Le_i = \rho D_i c_p / \lambda$ , Eqs. (18) and (20) become (with thin flame approximations)

$$\frac{d^2}{d\eta^2} (Le_i Y_i) + \frac{1}{\eta} \left( 1 - \frac{1}{Le_i} \right) \frac{d}{d\eta} (Le_i Y_i) = 0 \quad (21)$$

$$\frac{d^2 T}{d\eta^2} + \frac{dT}{d\eta} \left[ \frac{d}{d\eta} (\ln c_p) + \sum_{i=1}^4 Le_i \frac{c_{pi}}{c_p} \frac{dY_i}{d\eta} \right] = 0. \quad (22)$$

### Boundary Conditions

In the transformed coordinates, the continuity of mass flux of species  $i$  and of heat flux at the surface can be written as

$$\eta \frac{dY_i}{d\eta} \Big|_{\eta_s} = \frac{Y_i^+ - Y_i^-}{Le_i}, \quad (23)$$

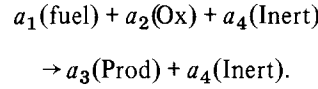
$$\eta \frac{dT}{d\eta} \Big|_{\eta_s} = \frac{Q}{c_p} \quad \text{where} \quad Q = L + c_c (T_s - T_0). \quad (24)$$

Here  $L$  is the latent heat of evaporation and the second term in  $Q$  constitutes the heat required to rise the temperature of the liquid from  $T_0$  to  $T_s$ .

At the flame zone, the thin-flame approximations lead to

$$\begin{aligned} Y_1 = 0 = Y_2 \quad \text{at} \quad \eta = \eta_f, \\ \frac{dY_1}{d\eta} \Big|_{\eta_f^-} = \frac{Le_2}{Le_1} \frac{a_1}{a_2} \frac{dY_2}{d\eta} \Big|_{\eta_f^+} \\ = \frac{Le_3}{Le_1} \frac{a_1}{a_3} \frac{dY_3}{d\eta} \Big|_{\eta_f^+}, \\ c_p \frac{dT}{d\eta} \Big|_{\eta_f^-} = - \sum_{i=1}^4 Le_i h_i \frac{dY_i}{d\eta} \Big|_{\eta_f^+}, \end{aligned} \quad (25)$$

where  $a_i$  are the stoichiometric coefficients in the single step reaction:



At large distance from the droplet:

$$\eta = 1: \quad Y_2 = \beta, \quad Y_3 = 0 \quad \text{and} \quad T = T_\infty. \quad (26)$$

The liquid-vapour equilibrium condition at the surface (Eq. 16) provides another condition.

### Solutions

Equation (21) can be solved for concentration profiles by making use of appropriate boundary conditions.

$$\left. \begin{aligned} Y_1 = 1 - (\eta/\eta_f)^{1/Le_1}, \quad Y_2 = 0 \\ Y_3 = (s+1)[(1+\beta/s)^{Le_2/Le_3} - 1] \\ \quad \times \eta^{1/Le_3} \end{aligned} \right\} \eta_s \leq \eta \leq \eta_f,$$

$$\left. \begin{aligned} Y_1 = 0, \\ Y_2 = \frac{\beta[1 - (\eta/\eta_f)^{1/Le_2}]}{[1 - (1/\eta_f)^{1/Le_2}]} \\ Y_3 = (s+1)(1 - \eta^{1/Le_3}) \end{aligned} \right\} \eta_f \leq \eta \leq 1,$$

$$\begin{aligned} Y_4 = 1 - Y_1 - Y_2 - Y_3 \quad \text{at any} \quad \eta, \\ \eta_f = 1/(1+\beta/s)^{Le_2}. \end{aligned} \quad (27)$$

The temperature profile can be obtained by solving Eq. (22) with conditions (24-26). We get

$$T = T_s + (T_f - T_s) \frac{I_1(\eta)}{I_1(\eta_f)} \quad \eta_s \leq \eta \leq \eta_f,$$

$$= T_f + (T_\infty - T_f) \frac{I_2(\eta)}{I_2(1)} \quad \eta_f \leq \eta \leq 1, \quad (28)$$

and

$$T_f = \left\{ \frac{T_\infty}{I_2(1)} + \frac{T_s}{I_1(\eta_f)} \exp [P(\eta_s, \eta_f)] + \frac{1}{\eta_f a_1} \right. \\ \left. \times (a_1 h_{1f} + a_2 h_{2f} + a_3 h_{3f}) \right\} \div \left\{ \frac{1}{I_2(1)} \right. \\ \left. + \frac{1}{I_1(\eta_f)} \exp [P(\eta_s, \eta_f)] \right\}, \quad (29)$$

where

$$I_1(\eta) = \int_{\eta_s}^{\eta} \frac{1}{c_p} \exp [P(\eta_s, \eta)] d\eta,$$

and

$$I_2(\eta) = \int_{\eta_f}^{\eta} \frac{1}{c_p} \exp [P(\eta_f, \eta)] d\eta. \quad (30)$$

In the above expressions  $P(\eta_1, \eta_2)$  has been written for

$$P(\eta_1, \eta_2) = - \int_{\eta_1}^{\eta_2} \sum_{i=1}^4 \frac{c_{pi}}{c_p} \text{Le}_i \frac{dY_i}{d\eta} d\eta.$$

Also, from Eqs. (24) and (28) we get

$$\eta_s = \frac{QI_1(\eta_f)}{T_f - T_s}. \quad (31)$$

### Retransformation into $r$ -coordinate

From the transformation

$$\eta = \exp \left[ \int \frac{\dot{m}}{4\pi r^2} \frac{c_p}{\lambda} dr \right],$$

we can write

$$\frac{\dot{m}}{4\pi r^2} dr = \frac{\lambda}{c_p} \frac{d\eta}{\eta},$$

which on integration between  $r$  and  $\infty$  leads to

$$\frac{\dot{m}}{4\pi r} = J(\eta) \quad \text{where} \quad J(\eta) = \int_{\eta}^1 \frac{\lambda}{c_p} \frac{d\eta}{\eta}. \quad (32)$$

Thus we have

$$r/r_s = J(\eta_s)/J(\eta), \quad (33)$$

$$d_f/d_s = J(\eta_s)/J(\eta_f); \quad K = \frac{8}{\rho_c} J(\eta_s). \quad (34)$$

Equations (27)–(34) constitute the set of implicit relations giving all the combustion parameters. Making use of  $c_p(Y_i, T)$ , first  $\eta_s$  and  $T_f$  can be obtained by an iterative procedure with initial approximations of  $T_s$ ,  $T_f$  and  $\eta_s$ . Retransformation into  $r$ -coordinate involves variation in  $\lambda$  also. Numerical calculations have been done for the benzene-air system. Five species ( $\text{C}_6\text{H}_6$ ,  $\text{O}_2$ ,  $\text{N}_2$ ,  $\text{CO}_2$ ,  $\text{H}_2\text{O}$ ) are considered to be in the field.  $c_{pi}$  are obtained from a curve fit of the data given by Svehla [29]. The thermal conductivity of the mixture is estimated by the standard procedure outlined in Ref. [33] with the molecular properties taken from Ref. [29].

### Results and Discussion

The spatial variations of temperature and the quantities  $c_p$ ,  $\lambda$  and  $\lambda/c_p$  in  $\eta$ -coordinate are shown in Fig. 6 for the case of  $\text{Le}_1 = \text{Le}_2 = 1.0$ . It may be seen that the variation of  $\lambda/c_p$  is very large in the field. As a result, the choice of  $(\lambda/c_p)_{av}$  becomes rather indeterminate if the SQST is used for predicting  $K$ . The expression for  $J(\eta_s)$  (Eq. 32), which is required in evaluating the burning constant  $K$ , suggests that the weightage for  $\lambda/c_p$  values close to the surface is large. The  $c_p$  profile exhibits an interesting feature in the occurrence of the peak being decidedly inside the flame rather than at the position of maximum temperature. This trend is the result of two opposing effects, namely the increasing temperature with  $\eta$  and the decreasing concentration of the fuel which at any temper-

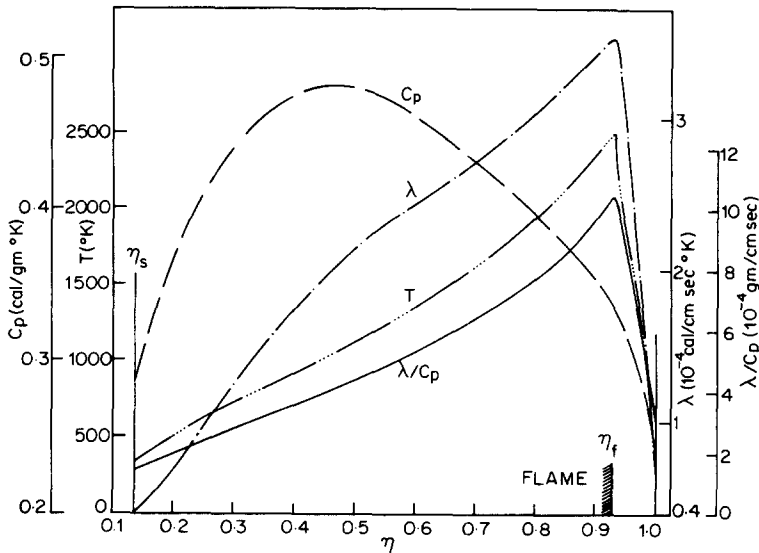


Fig. 6. Variations of  $T$ ,  $c_p$ ,  $\lambda$  and  $\lambda/c_p$  with  $\eta$  ( $Le_1 = Le_2 = 1.0$ )—variable property analysis.

ature has a higher  $c_{p_i}$  than other species (see Ref. 34 for similar observations).

The relations (29) and (34) predicts the values of “observables”,  $K$ ,  $d_f/d_s$  and  $T_f$ , without any uncertainty. Table 2 contains the results obtained by the different approximations of the present analysis. In the constant property approximation the constant value of  $\lambda$  ( $= 1.2 \times 10^{-4}$ ) chosen such that the prediction of  $K$  is realistic, occurs at a point where temperature is only  $670^\circ\text{K}$ . This is much below the arithmetic mean of surface and flame temperatures. Also, the location of this temperature is close to the surface as expected. Table 2 also demonstrates that the improvement in the prediction of  $d_f/d_s$  is significant when variable  $c_p$  and  $\lambda$  are employed. The prediction of  $K$  ( $= 0.72 \text{ mm}^2/\text{sec}$ ) agrees with the experimental

observations fairly well and the predicted flame temperature is same as the adiabatic flame temperature (compare with Table 1). However, the values of  $d_f/d_s$  and  $T_f$  are still larger than the experimentally observed values. Further improvements of the theoretical predictions are called for.

**Effect of Lewis Numbers**

By the definition of  $Le_i$  ( $= \rho D_i c_p / \lambda$ ), the variation of  $Le_i$  implies changes in the diffusion coefficient of species  $i$  in the mixture of gases. The results of Mukunda et al. [34] show that the Lewis numbers based on binary diffusion coefficients are different from unity in the major part of the field in a propane-air diffusion flame. Typically,  $Le_1$  is in the range 1.0–3.0 and  $Le_2$  around 1.1. The numerical

**TABLE 2**  
Comparison of Various Approximations in the Analysis ( $Le_1 = Le_2 = 1.0$ )

	$\lambda$ constant <sup>a</sup> $c_p$ constant <sup>b</sup>	$\lambda$ variable $c_p$ constant	$\lambda$ constant $c_p$ variable	$\lambda$ variable $c_p$ variable
$K$ ( $\text{mm}^2/\text{sec}$ )	0.7193	1.1102	0.5431	0.7239
$d_f/d_s$	28.303	23.868	20.910	15.359
$T_f$ ( $^\circ\text{K}$ )	2548	2548	2506	2506

<sup>a</sup> constant  $\lambda = 1.2 \times 10^{-4}$  chosen such that the SQST predicts realistic  $K$ .

<sup>b</sup> constant  $c_p = 0.304$  chosen such that the SQST correctly predicts adiabatic flame temperature.

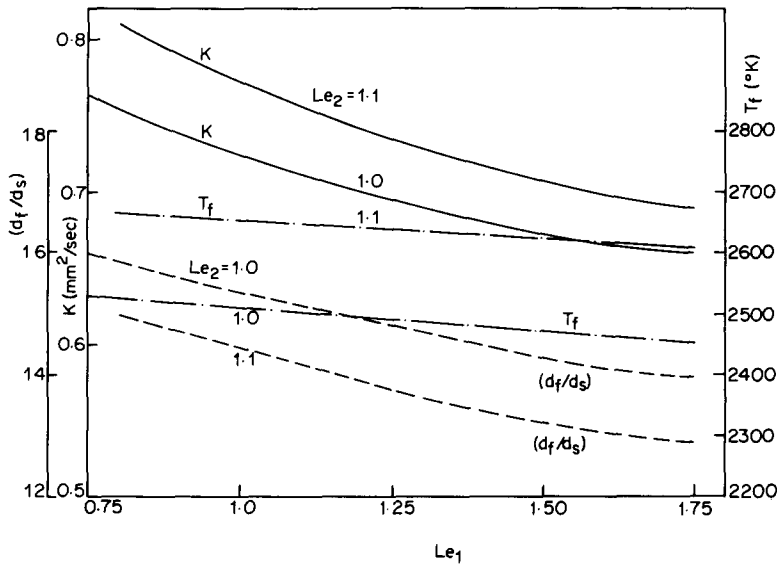


Fig. 7. Effect of Lewis numbers,  $Le_1$  and  $Le_2$  on combustion parameters.

calculations which examine the effect of variation of  $Le_1$  and  $Le_2$  from unity are presented in Fig. 7.

The quantities  $K$  and  $d_f/d_s$  decrease with an increase in  $Le_1$  and the effect on  $T_f$  is only marginal. One would expect from a physical picture that as  $Le_1$  increases (i.e., diffusion of fuel is faster), the burning rate would increase and as a consequence the flame would move away from the droplet. But the present results show a reverse trend. It may be noted that the arguments based on normal diffusion may not be valid in the present case. The interdependency of  $I_1(\eta_f)$  and  $\eta_s$  (Eqs. 30 and 31) produces the above trend of  $\eta_s$  increasing with  $Le_1$  and the subsequent reduction of  $K$  and  $d_f/d_s$  with  $Le_1$ .

The effect of increasing  $Le_2$  is to increase  $K$  and  $T_f$  and to reduce  $d_f/d_s$ . All three parameters have a greater sensitivity to  $Le_2$  than to  $Le_1$ . Although the increase of  $Le_2$  produces favourable effects on  $K$  and  $d_f/d_s$ , it increases the value of  $T_f$  which results in a greater deviation from experimental observations. Since the realistic values of  $Le_1$  and  $Le_2$  are approximately 1.5 and 1.1, it is thought that  $T_f$  must be lowered by including kinetic effects if all three characteristics are to be realistic.

#### An Approximation to Kinetic Effects

Some of the seemingly realistic values of  $d_f/d_s$  have been obtained by the choice of low stoichiometric ratio by earlier investigators [31, 32]. A few experimental observations suggest that complete oxidation of the fuel may not take place at the flame zone.

The soot formation during combustion of droplets [5] and the presence of significant amounts of carbon monoxide even beyond the diffusion flame zone (see for instance, Ref. 35) are definite indications of  $(O/F)$  being lower than stoichiometric at the flame zone.

The introduction of  $(O/F)$  lower than the stoichiometric value is contradictory to the theory using a single-step reaction with thin-flame kinetics. It is used here essentially to approximate the kinetic effects. The use of lower  $O/F$  calls for changes in thermal properties of the system.

Table 3 summarizes the reaction schemes and results of calculations made using  $(O/F)$  slightly lower than stoichiometric. It is evident that  $T_f$  approaches the observed flame temperatures with simultaneous improvement in the prediction of  $d_f/d_s$ . The choice of  $O/F < s$  causes the burning constant to decrease by a small amount.

TABLE 3

Effect of  $O/F$  at the Flame on Combustion Parameters ( $Le_1 = 1.5$ ,  $Le_2 = 1.1$ )

$O/F$	3.077	2.667	2.4615
Reaction products per mole of $C_6H_6$	$6 CO_2 + 3 H_2O$	$4 CO_2 + 2 CO + 3 H_2O$	$3 CO_2 + 3 CO + 3 H_2O$
$H$ (cal/g)	9700	7980	7110
$K$ ( $mm^2/sec$ )	0.7061	0.6873	0.6685
$d_f/d_s$	13.082	11.5685	10.636
$T_f$ ( $^{\circ}K$ )	2622	2460	2373

## CONCLUSIONS

The discrepancies between experimental results and the SQST predictions cannot be explained by unsteady effects alone. The unsteady effects last only through 20–25% of the total life of the droplet at the end of which time a quasi-steady state prevails. The transient analysis predicts the movement of the flame reasonably. The experimentally observed  $d^2$ -law appears to be due to the prevailing quasi-steady state.

Consideration of the detailed variation of  $c_p$  and  $\lambda$  in the field seems to clarify many discrepancies. The studies made in this regard lead us to the following conclusions for the process of combustion of a bipropellant droplet in an oxidising atmosphere without convection.

(1) The burning constant can be predicted accurately, primarily by including  $\lambda$  and  $c_p$  as functions of concentrations and temperature.

(2) The flame temperature can be meaningfully predicted by including the condition of incomplete combustion or low  $O/F$ .

(3) The prediction of  $d_f/d_s$  demands, in addition to the above two refinements, the introduction of realistic values of Lewis numbers  $Le_1$  and  $Le_2$ .

These predictions are not likely to be affected by unsteadiness, though the nature of variation from steady values may be affected. A combination of the two analyses presented in this paper, namely unsteady analysis and variable property analysis will prove useful in obtaining realistic predictions of the variation of  $d_f/d_s$ .

## NOMENCLATURE

$a$	Stoichiometric coefficient
$B$	Transfer number, defined in the text
$c_c$	Specific heat of liquid
$c_p$	Constant pressure specific heat in gas phase
$d$	Diameter
$D$	Diffusion coefficient
$f(t, r_s)$	Term representing condensed phase Unsteadiness (Eq. 15)
$h$	Enthalpy
$h^0$	Heat of formation
$h_s$	Sensible enthalpy
$H$	Heat of combustion per gm. fuel
$I_1(\eta), I_2(\eta)$	Integrals defined in Eq. (30)
$K$	Burning constant = $-(d/dt)(d_s^2)$
$L$	Latent heat of vaporisation
$Le$	Lewis number ( $=\rho D c_p / \lambda$ )
$\dot{m}$	Mass burning rate
$Q$	Effective heat of vaporisation
$r$	Radial coordinate, radius
$R$	Universal gas constant
$s$	Stoichiometric ratio
$t$	Time
$t_b$	Total burning time
$T$	Temperature
$T_b$	Boiling point of the liquid
$v$	Radial convective velocity
$Y$	Mass fraction
$\alpha$	Thermal diffusivity
$\beta$	Oxidiser mass fraction in the surrounding medium
$\eta$	Transformed radial coordinate
$\lambda$	Thermal conductivity
$\rho$	Density

$\dot{w}'''$  Mass consumption rate/unit volume

### Subscripts

*c* Condensed phase  
*f* At the flame  
*g* Gas phase  
*i* Species (1-fuel, 2-oxidiser, 3-products, 4-inert)  
*o* Initial state  
*s* At the surface  
 $\infty$  Ambient condition  
 ref Reference

### REFERENCES

- Williams, A., *Combust. Flame* 21, 1 (1973).
- Hedley, A. B., Nuruzzaman, A. S. M. and Martin, G. F., *J. Inst. Fuel* 44, 38 (1971).
- Krier, H. and Foo, C. L., *Oxidation and Combustion Reviews* 6, 111 (1973).
- Godsave, G. A. E., *Fourth Symposium (International) on Combustion* Williams and Wilkins, 1953, p. 818.
- Kobayasi, K., *Fifth Symposium (International) on Combustion* Reinhold, 1955, p. 141.
- Law, C. K. and Williams, F. A., *Combust. Flame* 19, 393 (1972).
- Aldred, J. W. and Williams, A., *Combust. Flame* 10, 396 (1966).
- Brzustowski, T. A. and Natarajan, R., *Can. J. Chem. Eng.* 44, 194 (1966).
- Spalding, D. B., *Fourth Symposium (International) on Combustion* Williams and Wilkins, 1953, p. 847.
- Aldred, J. W., Patel, J. C. and Williams, A., *Combust. Flame* 17, 139 (1971).
- Wise, H., Lorell, J. and Wood, B. J., *Fifth Symposium (International) on Combustion* Reinhold, 1955, p. 132.
- Isoda, H. and Kumagai, S., *Sixth Symposium (International) on Combustion* Reinhold, 1957, p. 726.
- Isoda, H. and Kumagai, S., *Seventh Symposium (International) on Combustion* Butterworths, 1959, p. 523.
- Kumagai, S., Sakai, T. and Okajima, S., *Thirteenth Symposium (International) on Combustion* The Combustion Institute, 1971, p. 779.
- Okajima, S. and Kumagai, S., *Fifteenth Symposium (International) on Combustion* The Combustion Institute, 1975, p. 401.
- Lorell, J., Wise, H. and Carr, R. E., *J. Chem. Phys.* 25, 325 (1956).
- Kassoy, D. R. and Williams, F. A., *Phys. Fluids* 11, 1343 (1968).
- Spalding, D. B., *ARS J.* 29, 828 (1959).
- Chervinsky, A., *Israel J. Tech.* 7, 35 (1969).
- Williams, F. A., *J. Chem. Phys.* 33, 133 (1960).
- Kotake, S. and Okazaki, T., *Intern. J. Heat Mass Transfer* 12, 595 (1969).
- Hubbard, G. L., Denny, V. E. and Mills, A. F., *Intern. J. Heat Mass Transfer* 18, 1003 (1975).
- Waldman, C. H., *Fifteenth Symposium (International) on Combustion* The Combustion Institute, 1975, p. 429.
- Raghunandan, B. N., *Diagnostic Studies on the Combustion of Liquid and Polymer Spheres*. Ph.D. Thesis, Indian Institute of Science, Bangalore, 1976.
- Wise, H. and Ablow, C. M., *J. Chem. Phys.* 27, 389 (1957).
- Hall, A. R., *Seventh Symposium (International) on Combustion* Butterworths, 1959, p. 399.
- Goldsmith, M. and Penner, S. S., *Jet Propulsion* 24, 245 (1954).
- Penner, S. S., *Chemistry Problems in Jet Propulsion* Pergamon (1957), pp. 276-291.
- Svehla, R. A., *Estimated Viscosities and Thermal Conductivities of Gases at High Temperatures* NASA TR R-132, 1962.
- Williams, F. A., *Combustion Theory* Addison Wesley 1965, pp. 47-57.
- Kassoy, D. R. and Williams, F. A., *AIAA J.* 6, 1961 (1968).
- Peskin, R. L. and Wise, H., *AIAA J.* 4, 1646 (1966).
- Hirshfelder, J. O., Curtiss, C. F. and Bird, R. B., *The Molecular Theory of Gases and Liquids* John Wiley and Sons Inc. 1954.
- Mukunda, H. S., Marathe, A. G. and Ramani, N., *Analysis of Variation of Thermodynamic and Transport Properties in Flames* HMT-45-71, First National Heat and Mass Transfer Conference, Indian Institute of Technology, Madras, 1971.
- Otsuka, Y. and Niioka, T., *Combust. Flame* 21, 163 (1973).

Received 25 January 1977; revised 14 March 1977